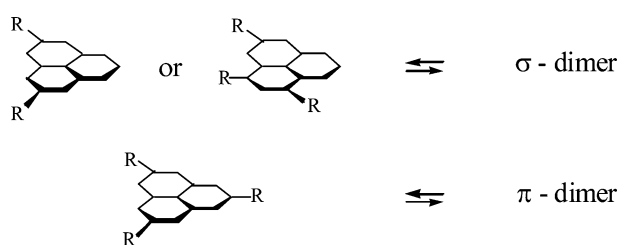# JOC*Article*

Steric Modulations in the Reversible Dimerizations of Phenalenyl Radicals via Unusually Weak Carbon-Centered π- and σ-Bonds

V. Zaitsev, S. V. Rosokha, M. Head-Gordon, and J. K. Kochi*

Departments of Chemistry, University of Houston, Houston, Texas 77204-5003, and University of California, Berkeley, California 94720

jkochi@uh.edu

Spontaneous self-associations of various tricyclic phenalenyl radicals lead reversibly to either π- or σ-dimers, depending on alkyl-substitution patterns at the α- and β-positions. Thus, the sterically encumbered all-β-substituted tri-*tert*-butylphenalenyl radical ($2^{\bullet}$) affords only the long-bonded π-dimer in dichloromethane solutions, under conditions in which the parent phenalenyl radical ($1^{\bullet}$) leads to only the σ-dimer. Further encumbrances of $1^{\bullet}$ with a pair of α, β- or β, β- *tert*-butyl substituents and additional methyl and ethyl groups (as in sterically hindered phenalenyl radicals $3^{\bullet} - 6^{\bullet}$) do not inhibit σ-dimerization. ESR spectroscopy is successfully employed to monitor the formation of both diamagnetic (2-electron) dimers; and UV−vis spectroscopy specifically identifies the π-dimer by its intense near-IR band. The different temperature-dependent spectral (ESR and UV−vis) behaviors of these phenalenyl radicals allow the quantitative evaluation of the bond enthalpy of 12 ± 2 kcal mol^{-1} for σ-dimers, in which the unusually low value has been theoretically accounted for by the large loss of phenalenyl (aromatic) π-resonance energy attendant upon such bond formation.

Introduction

Most organic (hydrocarbyl) free radicals are characterized by fast, diffusion-controlled (bimolecular) self-associations that occur with no or little activation energy.[1] For planar unsaturated species such as allyl radicals, symmetry considerations point to basically two types of facile intermolecular interactions designated as π- and σ-modes, e.g.[2]
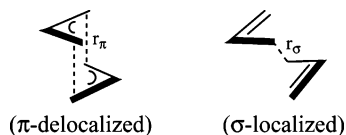
Although σ-interactions leading to covalent r_{σ} binding are by far the more common, there is recent experimental evidence that π-interactions can lead to long-bonded (delocalized) dimeric intermediates with wide r_{π} separations.[3,4]

The quantitative assessment of such a π versus σ dichotomy requires a common hydrocarbon framework in which both binding modalities are experimentally and simultaneously accessible. Thus, to address this problem directly, we now focus on the tricyclic phenalenyl radical ($C_{13}H_9^{\bullet}$)[5] for three important

(1) See, e.g.: (a) Benson, S. W. *Adv. Photochem.* **1964**, *2*, 1. (b) Nonhebel, D. C.; Walton, J. C. *Free-Radical Chemistry*; Cambridge University Press: Cambridge, 1974. (c) Ingold, K. U. In *Free Radicals*; Kochi, J. K., Ed.; Wiley: New York, 1973; Vol. 1, p 37ff.
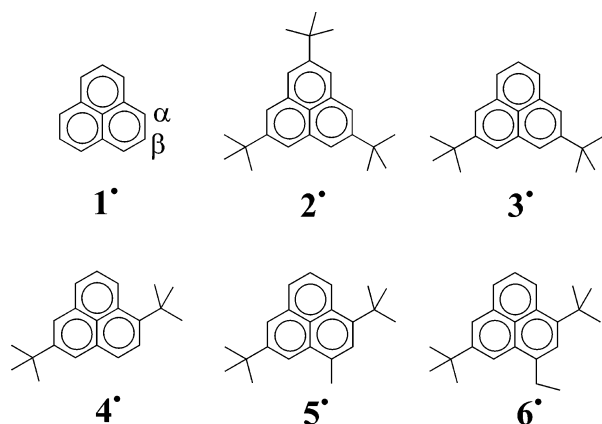
(2) As isomeric *syn* and *anti* forms. Note an analogous dichotomy is equally applicable to the well-known self-associations of such delocalized radicals as benzyl and cyclopentadienyl to the σ-dimers (diphenylethane and cyclopentadienylcyclopentadiene), but for which the π-forms as empty "sandwich" structures [e.g., ferrocene without iron(0)!] are as yet unknown.

(3) (a) Novoa, J. J.; Lafuente, P.; Del Sesto, R. E.; Miller, J. S. *Angew. Chem., Int. Ed.* **2001**, *40*, 2540. (b) Lu, J.-M.; Rosokha, S. V.; Kochi, J. K. *J. Am. Chem. Soc.* **2003**, *125*, 12161. (c) Jung, Y.; Head-Gordon, M. *Phys. Chem. Chem. Phys.* **2004**, *6*, 2008.

(4) (a) Chi, X.; Itkis, M. E.; Patrick, B. O.; Barklay, T. M.; Reed, R. W.; Oakley, R. T.; Cordes, A. W.; Haddon, R. C. *J. Am. Chem. Soc.* **1999**, *121*, 10395. (b) Chi, X.; Itkis, M. E.; Kirschbaum, K.; Pinkerton, A. A.; Oakley, R. T.; Cordes, A. W.; Haddon, R. C. *J. Am. Chem. Soc.* **2001**, *123*, 4041. (c) Itkis, M. E.; Chi, X.; Cordes, A. W.; Haddon, R. C. *Science* **2002**, *296*, 1443.

CHART 1

the same wide π-separation of phenalenyl moieties (Figure 1), which pertains independent of the *tert*-butyl groups; thus, $r_\pi = 3.2$ Å accurately identifies the unusually long π-bond inherent to the parent phenalenyl π-dimer (π-1_2).[11] On the other hand, the unambiguous identification of phenalenyl σ-dimer (σ-1_2) still remains somewhat problematic. For example, the earliest (chemical) studies suggest qualitatively the facile occurrence of σ-dimerization based on the isolation of dinuclear byproducts such as peropyrene, etc., but no pure σ-dimer can be isolated for definitive structure analysis.[5] Subsequent spectroscopic studies establish phenalenyl radical as an odd-alternant hydrocarbon and ascribe the marked temperature-dependent attenuation of the ESR signals to the reversible formation of the putative (diamagnetic) σ-dimer.[6] Most recently, quantitative ESR studies confirm the phenalenyl dimerization to occur reversibly in carbon tetrachloride and toluene solutions,[12] but the direct relationship of the measured enthalpy change of $-\Delta H_D = 10-11$ kcal mol^{-1} to the dissociation energy of a newly formed σ-bond remains uncertain. Since the latter represents an unusually low value for the homolytic scission of a $C(sp^3)-C(sp^3)$ single bond, our attention is now directed toward the unambiguous proof, identification, and understanding of the σ-dimerization process. Owing to the thermal lability of the σ-dimer that precludes any direct experimental approach to structure elucidation, we must perforce rely on indirect spectroscopic methods for structure proof. Accordingly in this study, we show how the critical placement of a pair of *tert*-butyl groups provides the delicate steric modulation sufficient to separate the π- and σ-binding modes for ESR and UV−vis observation and analysis, especially as they are coupled to our recent theoretical (quantum-chemical) calculations of the dimerization processes.[10]

FIGURE 1. Molecular structure of the π-dimer showing the staggered conformation of phenalenyl pairs separated by $r_\pi = 3.2$ Å.

reasons. First, phenalenyl radical is sufficiently persistent to allow quantitative spectroscopic (ESR and UV−vis) measurements in anaerobic solutions.[6] Second, there is some (qualitative) evidence for the independent existence of π- as well as σ-binding modes of phenalenyl radical.[7,8] Third, the aromatic (planar) character of phenalenyl radical allows the multiple placement of bulky *tert*-butyl substituents to selectively "tune" its steric properties over the three-ringed asymmetric (D_{3h}) skeleton,[9] as illustrated in Chart 1.

Previous experimental studies show that the presence of three *tert*-butyl substituents at each of the β-positions, as in radical **2**•, leads to the stable π-dimer with the unusually wide interannular (phenalenyl) separation of $r_\pi = 3.25$ Å established by X-ray crystallography.[7] Furthermore, molecular-orbital calculations indicate that *tert*-butyl groups enforce the staggered conformation to allow maximum overlap of the singly occupied orbitals (SOMO) centered at the six equivalent pairs of α-carbon centers and at the same time inhibit the competing formation of the σ-dimer[10a] Nonetheless, ab initio calculations confirm

Results and Discussion

1. Synthesis of Di-*tert*-butyl-Substituted Phenalenyl Radicals and Cations. The series of di-*tert*-butyl-substituted phenalenyl radicals in Chart 1 are prepared from the corresponding diamagnetic phenalene precursors by controlled (dehydro) oxidation with *p*-chloranil (CA) in degassed benzene solutions according to the procedure described earlier,[5,7] e.g.

$$2C_{13}H_{10} + CA \rightarrow 2C_{13}H_9{}^\bullet + H_2CA \qquad (1)$$

The phenalene precursor **3**-H is prepared from 2,7-di-*tert*-butylnaphthalene by the sequence of transformations outlined

(5) (a) Reid, D. H. *Chem. Ind.* **1956**, 1504. (b) Sogo, P. B.; Nakazaki, M.; Calvin, M. *J. Chem. Phys.* **1957**, *26*, 1343. (c) Reid, D. H. *Tetrahedron* **1958**, *3*, 339−352. (d) Reid, D. H. *Quart. Rev.* **1965**, *19*, 274.

(6) Gerson, F. *Helv. Chim. Acta* **1966**, *5*, 1463−1467.

(7) (a) Goto, K.; Kubo, T.; Yamamoto, K.; Nakasuji, K.; Sato, K.; Shiomi, D.; Takui, T.; Kubota, M.; Kobayashi, T.; Yakusi, K.; Ouyang, J. *J. Am. Chem. Soc.* **1999**, *121*, 1619. (b) Morita, Y.; Aoki, T.; Fukui, K.; Nakazawa, S.; Tamaki, K.; Suzuki, S.; Fuyuhiro, A.; Yamamoto, K.; Sato, K.; Shiomi, D.; Naito, A.; Takui, T.; Nakasuji, K. *Angew. Chem., Int. Ed.* **2002**, *41*, 1793. (c) Takano, Y.; Taniguchi, T.; Isobe, H.; Kubo, T.; Morita, Y.; Yamamoto, K.; Nakasuji, K.; Takui, T.; Yamaguchi, K. *J. Am. Chem. Soc.* **2002**, *124*, 11122.

(8) Paskovich, D. H.; Reddoch, A. H. *J. Am. Chem. Soc.* **1972**, *94*, 6938.

(9) Use of bulky *tert*-butyl groups to sterically inhibit σ-dimerization of aromatic radicals was first described by: Griller, D.; Ingold, K. U. *Acc. Chem. Res.* **1976**, *9*, 13.

(10) (a) Small, D.; Zaitsev, V.; Jung, Y.; Rosokha, S. V.; Head-Gordon, M.; Kochi, J. K. *J. Am. Chem. Soc.* **2004**, *126*, 13850−13858. (b) Essentially the same visible absorption band is calculated for the parent phenalenyl π-dimer (π-1_2) by high-level (quantum-mechanical) computational methodologies; and the strongly allowed electronic transition corresponds to the HOMO−LUMO transition from the delocalized ground-state over 12 π-centers. (c) Small, D.; Rosokha, S. V.; Kochi, J. K.; Head-Gordon, M. *J. Phys. Chem.,* in press. This reference also contains wave function-based coupled cluster and MP2 calculations with basis sets up to cc-pVTZ to allow for a reliable computational estimate of the bond dissociation energy of the phenalenyl sigma dimer of 16 kcal/mol in the gas phase. This allows an estimate of the loss of resonance energy in each phenalenyl unit of 34 kcal/mol upon sigma dimerization, associated with the rehybridization at the bridging carbons. Additionally, all calculations of the electronic absorption spectra were performed using time-dependent density functional theory with the B3LYP functional and the 6-31G* basis, which showed no bands of non-negligible intensity in the visible region, in striking contrast to the corresponding calculations on the π-dimer reported in ref 10a.
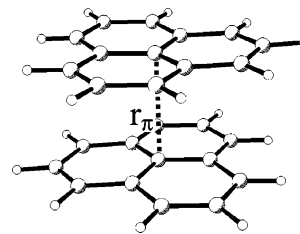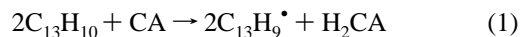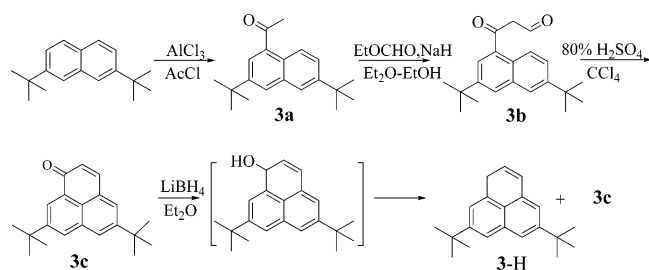
(11) Accordingly, the three *tert*-butyl groups in **2**• do not materially affect the energetics of the π-binding, and this conclusion is consistent with the wide separation of these groups (which exceeds the sum of their effective van der Waals radii) in the staggered π-2_2 ($r_\pi = 3.2$ Å). As such, the *tert*-butyl effect is manifested via the kinetic stability of the π-dimer; and this combination of 3 *tert*-butyl groups merely plays an inhibiting (steric) role on the competition from σ-bond formation.

(12) Zheng, S.; Lan, J.; Khan, S. I.; Rubin, Y. *J. Am. Chem. Soc.* **2003**, *125*, 5786.

SCHEME 1

TABLE 1. ESR Spectra of the Phenalenyl Radicals

radical	$a_H{}^a$ (G)	
3•	6.2 (6)	1.8 (1)
4•	6.2 (5)	1.9 (2)
5•	6.0 (4)	1.9 (1), 1.7 (1)
6•	6.1 (4)	1.9 (2)

[a] In parentheses: number of splitting protons.

in Scheme 1, and the phenalene isolated as colorless crystals consisting of a 2:2:1 mixture of three (hydro) isomers. Nonetheless, X-ray crystallography establishes the requisite near-planar (tricyclic) carbon skeleton shown in Figure S1 (Supporting Information), but most importantly, the chloranil oxidation converts 3-H to only a single isomer of 3• as a dark blue-green solid in 66% yield. All attempts to grow crystals of 3• suitable for X-ray crystallographic analysis have as yet been unsuccessful.

The diamagnetic phenalenyl cation 3^+ is prepared as deep red crystals of the tetrakis(perfluorophenyl)borate salt by hydride transfer from 3-H with the aid of triphenylcarbenium tetrakis-(perfluorophenyl)borate in dichloromethane under an argon atmosphere. X-ray crystallography establishes the triclinic crystals of 3^+ $(F_5C_6)_4B^-$ to consist of a single (planar) isomer with the expected tricyclic (carbon) skeleton shown in Figure S2 (Supporting Information).

The other phenylenes 4-H–6-H are similarly prepared from di-*tert*-butylnaphthalene followed by their conversion (with chloranil) to the corresponding phenalenyl radicals 4•–6•; details of the synthetic procedures, identification of all phenalene precursors, phenalenyl radicals and cations are presented in the Experimental Section.

2. Spectroscopic differentiation of π- versus σ-Dimerization. The experimental strategy for the unambiguous distinction between π- and σ-dimerization of phenalenyl radicals in solution is based on (1) first monitoring the temperature-dependent disappearance of phenalenyl radical by its diagnostic ESR spectrum and (2) then measuring the concomitant formation of π-dimer via its intense (UV−vis) absorption band at λ_{max} = 595 nm (ϵ_{max} 2 × 10^4 M^{-1} cm^{-1}).[10b] Thus, the ESR measurement will establish the overall (total) extent of the dimerization process irrespective of whether it results from π- and/or σ-binding modes; and the UV−vis measurement will specifically identify any contribution from the π-dimer since the σ-dimer is transparent in this spectral (>500 nm) region.[10c]

A. Monitoring the ESR Changes. The ESR spectrum of phenalenyl radical (1•) with $\langle g \rangle$ = 2.0031 consists of a well-resolved septet derived from two sets of hyperfine splittings of hfs = 6.3 G (6H) and 1.8 G (3H) for the α- and β-protons, respectively.[6,12] The latter set of hyperfine splittings are expectedly absent in 2,5,8-tri-*tert*-butylphenalenyl radical (2•), and the ESR spectrum with $\langle g \rangle$ = 2.0028 simply consists of a binomial septet with a single hfs of a_{6H} = 6.2 G.[7a] Moreover, the results in Table 1 show that the magnitudes of these α- and β-hyperfine splittings are essentially unaffected by the changing patterns of alkyl substitutions in phenalenyl radicals 3•–6•.

When the solution of 3-methyl-1,5-di-*tert*-butylphenalenyl radical in dichloromethane is progressively cooled, the line widths of the well-resolved spectrum of 5• remain unchanged, but the ESR intensity is reversibly attenuated (with temperature
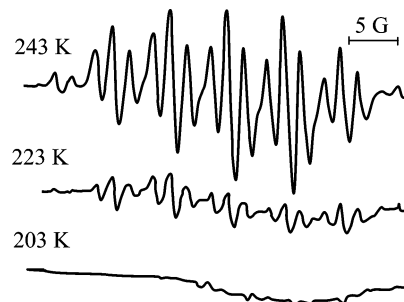

FIGURE 2. Temperature-dependent ESR spectrum of phenalenyl radical 5• (10 mM in dichloromethane) showing the dramatic concentration decrease due to dimer formation.
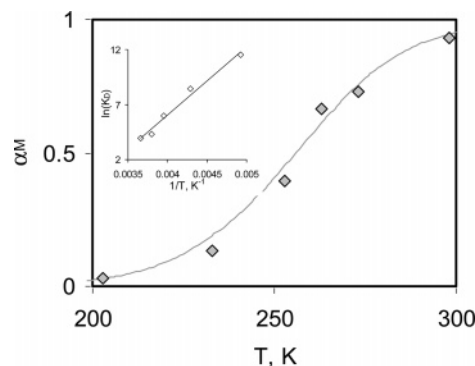

FIGURE 3. Sigmoidal temperature dependence of the monomer fraction α_M in the solution of the radical 5• in dichloromethane (c_0 = 5 mM). Inset: Linear (inverse) temperature dependence of the dimerization constant K_D.

variations) until it almost disappears completely at −70 °C, as illustrated in Figure 2. Double integration of the ESR spectrum (see Experimental Section) allows us to evaluate the fraction (α_M) of phenalenyl radical at various temperatures.

The dimerization constant for the equilibrium in eq 2 is calculated as $K_D = (1 - \alpha_M)/2C_0\alpha_M^2$

$$5• + 5• \underset{}{\overset{K_D}{\rightleftharpoons}} 5_2 \qquad (2)$$

where C_0 is the initial concentration of 5• in solution. The linear temperature dependence of log K_D affords the thermodynamic parameters as ΔH_D = −12 kcal mol^{-1} and ΔS_D = −42 eu, and the computer fit of both sets of experimental data according to eq 2 is shown by the light lines in Figure 3. It is thus important to emphasize that dimerization of the phenalenyl radical in eq 3 is reversible and complete at the lowest temperatures.

Application of the same experimental procedures to the parent phenalenyl radical 1• (Figure S3, Supporting Information), as well as to its sterically hindered tri-*tert*-butyl-substituted analogue 2•, yields dimerization constants that exhibit variations of over 4 orders of magnitude (Table 2). Further large variations are also seen for K_D of the methyl-*tert*-butyl-substituted 5• in

TABLE 2. Thermodynamic Parameters for the Formation of Diamagnetic Phenalenyl Dimers[a]

	$1^\bullet$	$2^{\bullet\ c}$	$5^\bullet$	$6^{\bullet\ d}$
K_D (M^{-1})[b]	$(3 \pm 1) \times 10^3$	0.15 ± 0.08	5 ± 1	0.6 ± 0.1
$-\Delta H_D$ (kcal mol^{-1})[e]	10.2	9.5	12.6	14.5
$-\Delta S_D$ (eu)[f]	18	36	39	50

[a] In CH_2Cl_2 unless otherwise noted. [b] 298 K. [c] From ref 10a. [d] In $CDCl_3$. [e] ± 1.0 kcal mol^{-1}. [f] ± 5 eu.

the comparison with the ethyl derivative $6^\bullet$. It is thus noteworthy that the thermodynamic parameters: ΔH_D and ΔS_D (Table 2, columns 3 and 4) show only modest variations that are singularly insensitive to steric differences. As such, let us now employ UV–vis spectroscopy to identify the role that π-dimers may (or may not) play in each of these dimerization processes.

B. UV–vis Identification of π- versus σ-Dimerization. The tri-*tert*-butylphenalenyl radical $2^\bullet$ is characterized in dichloromethane solution at 25 °C by its principal red absorption band ($\lambda_{max} = 540$ nm, $\epsilon \approx 10^2$ M^{-1} cm^{-1}), together with a very weak (broad) absorption at ~ 600 nm. Upon cooling the solution, only the low-energy band grows rapidly in intensity, and this dramatic spectral change is visually apparent by the transformation of the slightly pink color to an intense blue solution. Quantitative analysis of the ~600 nm absorbance[10a] together with the ESR behavior (Table 1) and previous X-ray structural data[7] allows (1) the unambiguous assignment of this additional intense absorption band ($\lambda_{max} = 595$ nm, $\epsilon = 2 \times 10^4$ M^{-1} cm^{-1}) to the π-dimer (π-$\mathbf{2_2}$), and (2) the evaluation of the dimerization constant of $K_D \approx 0.2$ M for the equilibrium in eq 3, together with the thermodynamic parameters $\Delta H_D = -8.8$ kcal mol^{-1} and $\Delta S = -33$ eu.[10a] Most importantly, the striking agreement of these π-dimerization constants with those determined from the ESR measurement in Table 2 (column 3) demonstrates that the UV–vis spectral changes accurately and quantitatively reflect the π-dimerization of $2^\bullet$ according to eq 3.

$$2^\bullet + 2^\bullet \overset{K_D}{\rightleftharpoons} \pi\text{-}2_2 \qquad (3)$$

By way of comparison, the UV–vis spectral changes upon lowering the temperature of the parent phenalenyl radical ($1^\bullet$) as well as the di-*tert*-butyl-substituted derivatives $3^\bullet$, $4^\bullet$, and $5^\bullet$ dissolved in dichloromethane (to afford pale blue solutions) exhibit no reversible change in the UV–vis spectra in the 550–650 nm region that is expected for the π-dimers. Aside from the local bands of the phenalenyl moiety at $\lambda \sim 540$–550 nm ($\epsilon \sim 10^2$ M^{-1} cm^{-1} vide supra), no significant additional absorption is apparent in these phenalenyl radicals, except for temperature-independent and weak (nondescript) absorptions at ~ 610 nm. Closer scrutiny of the latter in the case of methyl-di-*tert*-butylphenalenyl $5^\bullet$ is allowed by the identification of the strongly absorbing species 7 which is isolated (at low conversions) as a dark-blue diamagnetic crystal ($\lambda_{max} = 610$ nm, $\epsilon = 1.1 \times 10^5$ M^{-1} cm^{-1}). X-ray crystallographic analysis establishes 7 as the dehydrodimer,[13] the essentially planar structure of which is illustrated in Figure 4. (Note that π-conjugation at the pair of bridging centers of 7 is indicated by the close bond distances of 1.39 and 1.41 Å.)

The successful isolation and structural characterization of the dehydrodimer 7 suggests that the parent phenalenyl radical $1^\bullet$ as well as the di-*tert*-butyl derivatives $3^\bullet$, $4^\bullet$, and $5^\bullet$ are not quite as persistent as the di-*tert*-butyl analogue $2^\bullet$, and all are subject
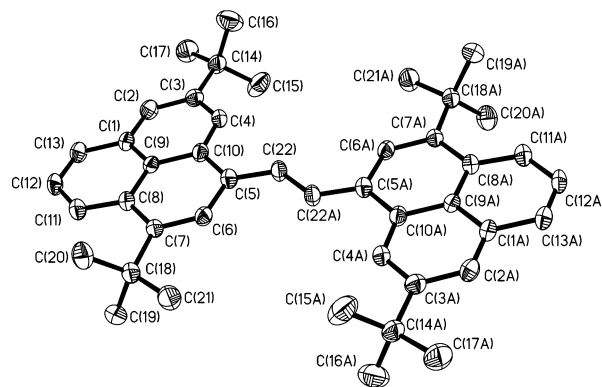
FIGURE 4. ORTEP diagram of the dehydrodimer 7 with all hydrogens omitted for clarity.

to suffer from some (minor extent) unavoidable and irreversible bimolecular processes. Nonetheless, when phenalenyl radicals $1^\bullet$, $3^\bullet$–$5^\bullet$ are carefully prepared, the combined ESR/UV–vis analyses establish the reversible σ-dimerization to be the principal pathway—without the incursion of π-dimerization (which is only observed with the sterically hindered tri-*tert*-butylphenalenyl radical $2^\bullet$). However, such bimolecular byproducts can be avoided entirely if some additional steric constraints are imposed, as in the slightly more hindered analogue ($6^\bullet$). Thus, 5 mM solutions of $6^\bullet$ in dichloromethane are practically colorless and show at room temperature only the local bands of the phenalenyl moiety with $\lambda \sim 550$ nm ($\epsilon \sim 10^2$ M^{-1} cm^{-1}). These solutions of $6^\bullet$ remain colorless even upon lowering the temperature to -90 °C, and electronic spectroscopy confirms that no new absorption band of the π-dimer appears in the vis–NIR region. Coupled with the ESR measurements in Table 2 (entry 4), the temperature-dependent equilibrium shift of $6^\bullet$ (solution is ESR-silent at -90 °C) must pertain to the sole formation of the colorless (diamagnetic) σ-dimer in potentially quantitative amounts.[14]

3. Steric Requirements for π-Dimerization. The foregoing alkyl-substitution patterns demonstrate that the pathway for σ-dimerization is consistently favored for the phenalenyl radicals depicted in Chart 1, except when the three β-positions are fully substituted with bulky *tert*-butyl groups. Thus, a more general question does arise: how important are steric effects in π-interactions between a pair of phenalenyl moieties? To address this question, we consider the direct association of a phenalenyl radical ($\mathbf{P}^\bullet$) with its diamagnetic cationic counterpart ($\mathbf{P}^+$), i.e.

(13) (a) For the observation of other byproducts containing two phenalenyl moieties, see Reid et al.[5] However, the temperature-dependent behavior suggests that 7 was generated independent of $5^\bullet$, and we speculate that it derived directly from $(5-H)^{+\bullet}$ during chloranil oxidation followed by rapid proton loss and dimerization of the benzylic radical. Further chloranil oxidation of the electron-rich dihydrodimer would lead to 7, the structure of which (Figure 4) is directly related to the similar dehydro derivative of α-methylphenalene synthesized earlier[13b] and shown below as a resonance hybrid with the (di)radicaloid form
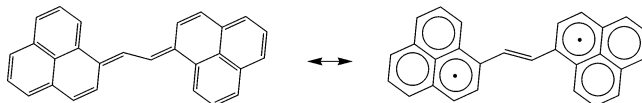
(b) Nakasuji, K.; Yoshida, K.; Murata, I. *J. Am. Chem. Soc.* **1982**, *104*, 1432.
(14) Thus, $6^\bullet$ offers the best possibility for the isolation (and structure determination) of a phenalenyl σ-dimer, provided its facile dissociation can be controlled.

$$\mathbf{P}^{\bullet} + \mathbf{P}^{+} \rightleftarrows \pi\text{-}\mathbf{P}_2^{+\bullet} \qquad (4)$$

for which the driving force for the formation of the dimeric cation-radical ($\mathbf{P}_2^{+\bullet}$) will be less than that for the phenalenyl dimer itself ($\mathbf{P}_2$) owing to one fewer bonding (HOMO) electron.

The formation of the dimeric cation-radical from the parent phenalenyl radical ($\mathbf{1}^{\bullet}$) and its cation ($\mathbf{1}^{+}$) is characterized by the appearance of an intense near-IR absorption band at $\lambda_{max} = 1700$ nm ($\epsilon \sim 1 \times 10^4$ M^{-1} cm^{-1}) as well as the ESR spectrum consisting of doubled lines with halved hyperfine splitting[8] that are diagnostic of the cofacial juxtaposition of two (equivalent) phenalenyl moieties π-bonded at the same wide separation of $r_{\pi} = 3.2$ Å.[10a,15,16]

Indeed, the addition of the 2,5-di-*tert*-butyl-substituted phenalenyl radical $\mathbf{3}^{\bullet}$ to a dichloromethane solution of the corresponding phenalenyl cation $\mathbf{3}^{+}$ results in the appearance of a strong NIR absorption band ($\lambda_{max} = 1750$ nm, Figure S4, Supporting Information) and doubled ESR spectrum in Figure 5 characteristic of the dimeric cation cation-radical (π-$\mathbf{3}_2^{+\bullet}$). By contrast, 3-ethyl-1,5-di-*tert*-butylphenalenyl radical ($\mathbf{6}^{\bullet}$) shows no evidence of forming the dimeric cation radical (π-$\mathbf{6}_2^{+\bullet}$) by the singular absence of any absorption in the 1000–3000-nm range, when it is exposed to its cationic counterpart ($\mathbf{6}^{+}$), i.e.

$$\mathbf{6}^{\bullet} + \mathbf{6}^{+} \neq \pi\text{-}\mathbf{6}_2^{+\bullet} \qquad (5)$$

Furthermore, ESR measurements also fail to detect any new absorption in the spectrum of radical $\mathbf{6}^{\bullet}$ when the cation $\mathbf{6}^{+}$ is added.[17a] As such, we conclude that (1) the association of radical $\mathbf{1}^{\bullet}$ with its closed-shell cation $\mathbf{1}^{+}$ (and $\mathbf{3}^{\bullet}$ with $\mathbf{3}^{+}$) leads to the formation of the π-bonded dimeric cation-radical, but (2) the pattern of alkyl substituents plays an important steric role since the combination of ethyl and a pair of *tert*-butyl groups in $\mathbf{6}^{\bullet}$ is sufficient to inhibit the formation of the stable (staggered) conformation shown in Figure 1.[17b]

4. Unusual Bond Enthalpies in π- and σ-Dimers. The energetics for the reversible dimerization of $\mathbf{2}^{\bullet}$ according to eq 3 establishes the bond enthalpy for the π-dimer as $\Delta H_{\pi} = 9.5$ kcal mol^{-1} in dichloromethane solution, which compares well with the value of 11 kcal mol^{-1} for the gas-phase dissociation calculated by ab initio (quantum-mechanical) methodologies.[10a]

By analogous comparisons, the bond enthalpies for the σ-dimers of $\Delta H_{\sigma} = 10$ and 12 kcal mol^{-1} evaluated for the parent phenalenyl radical (σ-$\mathbf{1}_2$) and the *tert*-butyl substituted analogue (σ-$\mathbf{5}_2$) in dichloromethane solution (Table 2) are essentially the same as the values of 9.8 and 11 kcal mol^{-1} previously evaluated for the parent $\mathbf{1}_2$ in carbon tetrachloride and toluene, respectively,[12] as well as the calculated bond

(15) (a) Lewis, I. C.; Singer, L. S. *Chem. Phys.* **1965** *43*, 2712. (b) Howarth, O. W.; Fraenkel, G. K. *J. Chem. Phys.* **1970**, *52*, 6258. (c) Lau, W.; Kochi, J. K. *J. Org. Chem.* **1986**, *51*, 1801. (d) Kochi, J. K.; Rathore, R, Le Magueres, P. *J. Org. Chem.* **2000**, *65*, 6826P.

(16) (a) Stenger-Smith, J. D.; Lenz, R. W.; Enkelmann, V.; Wegner G. *Macromol. Chem.* **1992**, *193*, 575. (b) Le Magueres, P.; Lindeman, S.; Kochi, J. K.; *J. Chem. Soc., Perkin Trans 2* **2001**, 1180.

(17) (a) However, careful examination of the ESR spectrum shows the progressive linebroadening of $\mathbf{6}^{\bullet}$ in the presence of added $\mathbf{6}^{+}$, which we tentatively ascribe to the facile (ET) self-exchange via either a very weakly bound π- or σ-associate ($\mathbf{6}_2^{+\bullet}$). (b) This raises the question as to whether a tri-alkyl(substitution) pattern consisting of 2,5-di-*tert*-butyl substituents together with a small alkyl substituent (such as a methyl or ethyl) at the 8-position would produce a phenalenyl system capable of accommodating *both* π- and σ-modes simultaneously in reversible competition with one another.
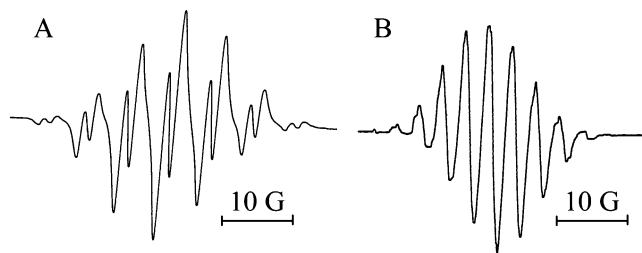
FIGURE 5. ESR spectrum of phenalenyl radical $\mathbf{3}^{\bullet}$ (A) and that of an equimolar mixture of $\mathbf{3}^{\bullet}$ and $\mathbf{3}^{+}$ showing the doubling of the number of hyperfine lines and halving of the splittings diagnostic of the dimeric cation radical $\mathbf{3}_2^{+\bullet}$ (B).
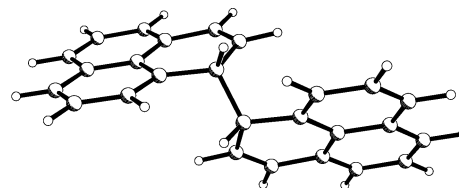

FIGURE 6. Calculated structure of the phenalenyl σ-dimer.

enthalpy of 16 kcal mol^{-1} for the gas-phase dissociation of σ-$\mathbf{1}_2$, the calculated structure of which is shown in Figure 6.[10c,18] Furthermore, the simple (global) average of $\Delta H_{\sigma} = 12 \pm 2$ kcal mol^{-1} (that does not distinguish between solution and gas-phase processes) is also essentially the same as the value of 14.5 kcal mol^{-1} measured for the highly hindered $\mathbf{6}_2$ (see Table 2, entry 4). On the other hand, these steric characteristics serve to strongly distinguish the various formation constants for σ-dimerization (see K_D in Table 2, for first, third and fourth entries). As such, we conclude that steric effects do not play a significant role in determining the σ-bond enthalpy.

It is noteworthy that the magnitudes of the bond enthalpies of 10 and 12 kal mol^{-1} estimated for the phenalenyl π- and σ-dimers are both so small. Indeed, theoretical calculations have shown that intermolecular associations lead to considerable loss of aromaticity of approximately 34 kcal mol^{-1} per phenalenyl moiety, or an overall loss of $\sim$ 70 kcal mol^{-1}, upon the formation of the σ-dimer.[10c] Such a large loss of resonance π-stabilization energy relative to the average carbon/carbon bond enthalpy of roughly 83 kcal mol^{-1} thus leaves only a small residual for ΔH_{σ}. The electronic basis for the small bond enthalpy of the widely separated π-dimer was discussed earlier in detail.[10a]

Summary and Conclusions

Spectroscopic (ESR, UV–vis) methodologies allow the structural identification of phenalenyl radicals $\mathbf{1}^{\bullet}$–$\mathbf{6}^{\bullet}$ (Chart 1), as well as the quantitative measurements of their distinctive conversions to diamagnetic (two-electron) dimers with unusual π- and σ-bonds. Steric modulations by judicious placement of two or more *tert*-butyl substituents alter the course from σ- to π-dimerization. Thus, the sterically encumbered 2,5,8-tri-*tert*-butylphenalenyl radical $\mathbf{2}^{\bullet}$ affords only the π-dimer (π-$\mathbf{2}_2$), whereas the parent phenalenyl radical ($\mathbf{1}^{\bullet}$) leads only to the

(18) It is noteworthy that the calculated phenalenyl σ-separation of $r_{\sigma} = 1.585 \pm 0.010$ Å in Figure 6 is slightly longer that the usual C(sp^3)−C(sp^3) bond length, but it is in strong accord with X-ray structural studies of σ-bonded phenalenyl moieties in spirobiphenalenyls (1.599 Å)[18b] and in copper complexes of azaphenalenyl σ-dimers (1.583 Å).[12] (b) Liao, P.; Itkis, M. E.; Oakley, R. T.; Tham, F. S.; Haddon, R. C. *J. Am. Chem. Soc.* **2004**, *126*, 14297.

σ-dimer (σ-**1₂**). Moreover, further substitutions of the latter with two additional *tert*-butyl and methyl or ethyl groups, as in **3•**–**6•**, are insufficient to alter this course. All dimerizations occur reversibly; and linear (inverse) temperature dependences of the dimerization constants (ln K_D) yield the thermodynamic parameters: $\Delta H \sim -12 \pm 2$ kcal mol^{-1} and $\Delta S \sim -30 \pm 10$ eu that are to within the experimented uncertainty, the same for both isomeric processes. Such an unusual (and unexpected) conclusion to more or less equate energetics of π-delocalized with σ-localized bindings follows from an overwhelming loss of π-aromatic-stabilization energy attendant upon σ-dimerization.

Experimental Section

Synthesis and Identification of Phenalene Precursor, Phenalenyl Radicals, and Cations. Phenalenyl radical **2•** was prepared by the oxidation of the corresponding phenalene with chloranil (2:1 molar ratio) via the modified literature method[7a] in benzene under air-free conditions, followed by evaporation and extraction with degassed pentane. Separation and evaporation (in vacuo) of the clear slightly blue-color pentane solution afforded radical **2•** as deep blue needles. Radical **1•** was prepared from the phenalene precursor (**1**–**H**) and chloranil in the similar way and was identified via its ESR spectra (Table 1). Tetrakis(perfluorophenyl)borate salt of cations **1⁺** and **2⁺** were prepared as described earlier.[10a] **2,5-Di-*tert*-butylphenalene (3**-H) was synthesized (Scheme 1) as follows. **3a.** AlCl₃ (2.8 g, 21 mmol) was added during 10 min to the stirred solution of 2,7-di-*tert*-butylnaphthalene[19] (4.0 g, 16.7 mmol) in 40 mL of acetyl chloride at 0 °C. After 10 min, the green reaction mixture was poured onto 300 g of ice. The resulting green solid was filtered, dried in air overnight and used for the next step without additional purification. Yield: 4.1 g (87%). ¹H NMR (CDCl₃): 1.41 (s, 9H); 1.44 (d, $J = 0.6$ Hz, 9H); 2.75 (d, $J = 0.6$ Hz, 3H); 7.64 (ddd, $J = 9.0, 2.0, 0.8$ Hz, 1H); 7.77 (d, $J = 1.1$ Hz); 7.91 (s, 1H); 7.95 (s, 1H); 8.58 (d, $J = 9.0$ Hz, 1H). MS (70 eV): 282 (45) [M⁺•]; 267 (100) [M⁺• − Me]. **3b.** EtOH (0.1 mL) was added to a stirred slurry of NaH (1.5 g, 38 mmol, 60% in oil) in 100 mL of diethyl ether, followed by the addition of a solution of 1-acetyl-3,6-di-*tert*-butyl-naphthalene **3a** (4.1 g, 15 mmol) in 30 mL of Et₂O and then EtOCHO (2.5 mL, 30 mmol). The reaction mixture was heated to reflux, and hydrogen evolution was observed after a short induction period. After 1 h of refluxing, most of the solid dissolved, gas evolution ceased, and the reaction mixture was quenched by careful addition of H₂O (1 mL, then 100 mL). The aqueous layer was separated, washed with Et₂O (2 × 30 mL), and acidified with a 2 M solution of HCl. Extraction with Et₂O (3 × 30 mL), drying of the combined extracts with MgSO₄, and evaporation of the solvent afforded diketone **3b** as a colorless oil, which was used for the next step without purification. Yield: 4.2 g (93%). ¹H NMR (CDCl₃): 1.42 (s, 9H); 1.43 (d, $J = 0.9$ Hz, 9H); 6.12 (dd, $J = 4.5, 0.6$ Hz, 1H); 7.62 (d, $J = 9.0$ Hz, 1H); 7.79 (s, 2H); 7.90 (s, 1H); 8.20 (d, $J = 4.2$ Hz,1H); 8.38 (d, $J = 9.0$ Hz, 1H). MS (70 eV): 310 (62) [M⁺•]; 295 (100) [M⁺• − Me]; 281 (9); 267 (58); 57 (50) [Bu⁺•]. **3c.** A solution of diketone **3b** (4.2 g, 13.5 mmol) in 15 mL of CCl₄ was added dropwise during 30 min to a vigorously stirred solution of 80% H₂SO₄ (100 mL) cooled in an ice bath. After 1 h, the deep red reaction mixture was poured onto ice (400 g). The yellow solid was separated by filtration, dried in air overnight and used for the next step without purification. Yield: 3.8 g (96%). Mp: 148−152 °C. ¹H NMR (CDCl₃): 1.46 (s, 9H); 1.48 (s, 9H); 6.74 (d, $J = 9.6$ Hz, 1H); 7.75 (d, $J = 9.6$ Hz, 1H); 7.80 (d, $J = 1.8$ Hz, 1H); 7.96 (d, $J = 1.8$ Hz,1H); 8.16 (d, $J = 1.8$ Hz, 1H), 8.70 (d, $J = 1.8$ Hz, 1H). MS (70 eV): 292(45) [M⁺•]; 277 (100) [M⁺•-Me]. **3-H.** LiBH₄ (100 mg, 7.2 mmol) was added during 5 min to the solution of enone **3c** (1.1 g, 3.8 mmol) in Et₂O

(100 mL), the mixture was stirred during 2 h, and then 0.5 mL of water was added. The precipitate was filtered off through MgSO₄, and the solvent was evaporated to afford a yellow residue (1.1 g), which was separated by chromatography on 16 g of silica gel. Evaporation of the first fraction (hexane, 150 mL) resulted in a white powder, which after recrystallization (EtOH/H₂O) afforded colorless plates of 2,5-di-*tert*-butylphenalene as a mixture (2:2:1) of three positional isomers (0.33 g, 31%,) of **3**-H. Mp: 86 C. ¹H NMR (CDCl₃): 1.222 and 1.225, 1.36 and 1.37, 1.38 and 1.39 (2:1:2) (s). Anal. Calcd for C₂₁H₂₆: C, 90.59; H, 9.41. Found: C, 90.38; H, 9.56. The structure of **3**-H was confirmed by X-ray analysis (Figure S1, Supporting Information). The second fraction (benzene, 100 mL) afforded the starting enone **3c** (0.40 g, 38%). **Radical 3•.** A solution of chloranil (50 mg, 0.20 mmol) in benzene (2.5 mL) was carefully degassed (by repeated freeze-and-pump cycles techniques), heated to 50 °C and added under argon to a solution of **3-H** (110 mg, 0.40 mmol) in benzene. A transient green color followed by a deep blue coloration appeared after dissolving the phenalene, and this was then followed by a precipitate. After 10 min, the solvent was evaporated, and the residue was extracted with degassed pentane (2 mL). Evaporation (in vacuo) of the clear blue pentane solution resulted in a blue oil which solidified spontaneously to a blue-green solid **3•** (66 mg, 66%). Mp: > 110 C dec. ESR (5 mM in PrNO₂): doublet of septets, $\alpha = 1.8$ G, $\alpha_1 = 6.2$ G. MS (70 eV): 278 (25) [M⁺• + 1]; 277 (30) [M⁺•]; 262 (35) [M⁺• − Me]; 247 (13) [M⁺• − 2Me]; 231(10); 221 (100); 205 (13); 191 (10); 165 (10); 57(8) [Bu⁺•]. **Cation 3⁺ B(C₆F₅)₄⁻.** Triphenylcarbenium tetrakis(perfluorophenyl)borate (from Asahi Glass Co., Ltd.) [300 mg (0.33 mmol in 2 mL of CH₂Cl₂)] was added to the solution of **3-H** (117 mg, 0.42 mmol) in 4 mL of CH₂Cl₂ under argon. Addition of 8 mL of hexane to the reaction mixture resulted in the precipitation of a red powder, which was separated and recrystallized from ether/hexane (1:2) to afford red crystals: yield 39%. ¹H NMR (CDCl₃): 1.60 (s, 18H); 8.35 (t, $J = 7.8$ Hz, 1H); 9.10 (d, $J = 7.8$ Hz, 2H); 9.18 (s, 2H); 9.22 (s, 2H). Anal. Calcd for C₄₅H₂₅BF₂₀: C, 56.51; H, 2.63. Found: C, 56.55; H, 2.59. The X-ray structure of **3⁺**B(C₆F₅)₄⁻ is shown in Figure S2 (Supporting Information). **1,5-Di-*tert*-butylphenalene (4-H)** was synthesized from 2,6-di-*tert*-butylnaphthalene via procedures similar to those in Scheme 1 (note that **4a**, **4b**, and **4c** designate the 1,5-di-*tert*-butyl-substituted analogues of **3a**, **3b**, and **3c**). **4a.** Green solid (yield: 1.2 g, 64%). ¹H NMR (CDCl₃): 1.42 (s, 9H); 1.44 (s, 9H); 2.77 (s, 3H); 7.61 (dd, $J = 8.7, 1.8$ Hz, 1H); 7.80 (d, $J = 8.7$ Hz, 1H); 7.89 (s, 1H); 7.97 (d, $J = 1.8$ Hz, 1H); 8.63 (s, 1H). MS (70 eV): 282 (54) [M⁺•]; 267 (100) [M⁺• − Me]. **4b.** Yellow oil, which solidified upon standing. Yield: 0.62 g (47%). ¹H NMR (CDCl₃): 1.40 (s, 9H); 1.42 (d, $J = 0.9$ Hz, 9H); 6.12 (d, $J = 4.5$ Hz); 7.60 (dd, $J = 8.4, 1.5$ Hz, 1H); 7.80 (d, $J = 8.4$ Hz, 1H); 7.86 (d, $J = 1.5$ Hz, 1H); 8.20 (d, $J = 4.2$ Hz, 1H); 8.38 (s, 1H). **4c.** Yellow solid. Yield: 0.61 g (98%). ¹H NMR (CDCl₃): 1.46 (s, 9H); 1.65 (s, 9H); 6.21 (d, $J = 10.5$ Hz, 1H); 7.71 (d, $J = 9.0$ Hz, 1H); 7.93 (d, $J = 9.0$ Hz, 1H); 8.10 (s, 1H); 8.54 (d, $J = 10.5$ Hz, 1H), 8.78 (s, 1H). MS (70 eV): 292 (45) [M⁺•]; 277 (100) [M⁺• − Me]. **4-H.** Colorless crystals, mixture of isomers. Yield: 0.14 g (25%). MS (70 eV): 278 (17) [M⁺•]; 277 (30) [M⁺• − 1]; 262 (64) [M⁺• − 1 − Me]; 247 (18) [M⁺• − 1 − 2Me]; 221(100) [M⁺• − 57]; 205 (13); 165 (10); 96 (10); 57 [Bu⁺•]. Radical **4•** was prepared by the reaction of **4-H** (250 mg, 0.89 mmol) with chloranil (110 mg, 0.45 mmol) in benzene (4 mL). Yield: 210 mg (84%). ESR (5 mM in pentane): triplet of sextets, $\alpha = 1.9$ G, $\alpha_1 = 6.2$ G (Figure S6, Supporting Information). MS (70 eV): 278 (16) [M⁺• + 1]; 277 (50) [M⁺•]; 262 (100) [M⁺• − Me]; 247 (18) [M⁺• − 2Me]; 221(45); 205 (25); 165 (10); 95(15); 57(5) [Bu⁺•]. Cation **4⁺** B(C₆F₅)₄⁻ was prepared by the reaction of **4-H** with triphenylcarbenium tetrakis(perfluorophenyl)borate. Orange-red crystals. Yield: 41%. ¹H NMR (CDCl₃): 1.59 (s, 9H); 1.89 (s, 9H); 8.31 (dd, $J = 7.5$ and 8.1 Hz, 1H); 8.42 (d, $J = 8.1$ Hz, 1H); 8.94 (d, $J = 8.4$ Hz, 1H); 9.00 (d, $J = 7.5$ Hz, 1H); 9.08 (br s, 2H); 9.86 (9.10 (d, $J = 7.8$ Hz, 2H); 9.18 (s, 2H); 9.86 (d, $J = 8.4$

(19) Koch, K. H.; Muellen, K. *Chem. Ber.* **1991**, *24*, 2091.

Hz, 1H). Anal. Calcd for $C_{45}H_{25}BF_{20}$: C, 56.51; H, 2.63. Found: C, 56.78; H, 2.50. The X-ray structure of $4^+B(C_6F_5)_4^-$ is shown in Figure S5 (Supporting Information). **3-Methyl-1,5-di-*tert*-butylphenalene (5-H)** was synthesized from 4-methyl-2,6-di-*tert*-butylnaphthalene via the procedure similar to those in Scheme 1. To synthesize 4-methyl-2,6-di-*tert*-butylnaphthalene, 1.2 mL of Br_2 (23 mmol) was added during 10 min to the solution of 2,6-di-*tert*-butylnaphthalene (4.8 g, 20 mmol) in CH_2Cl_2 (50 mL) at 0 °C. The reaction mixture was stirred for an additional 30 min, and evaporation of solvent gave 6.9 g of 3-bromo-2,6-di-*tert*-butyl-naphthalene as an oil. This oil was dissolved in 150 mL of THF, and 2.5 M BuLi in hexanes (10 mL, 25 mmol) was added dropwise at −78 °C. A yellow precipitate started to form after the addition of 7 mL of BuLi. The reaction mixture was stirred for 10 min at −78 °C, then 2.5 mL (26 mmol) of Me_2SO_4 was added for 10 min and resulted in the formation of a clear yellow solution. Finally, 1 mL of water was added, the solvent was evaporated in vacuo, and the residue was extracted with ether (3 × 30 mL). The combined ethereal extracts were washed with water and brine and filtered through a 1-cm pad of $MgSO_4$. Evaporation of the solvent led to an oil, which crystallized upon standing to afford large colorless needles. Yield of 4-methyl-2,6-di-*tert*-butylnaphthalene: 4.5 g (89%). ^{1}H NMR (CDCl$_3$): 1.41 (s, 9H); 1.44 (s, 9H); 2.71 (s, 3H); 7.39 (s, 1H); 7.55 (dd, J = 8.7, 2.1 Hz, 1H); 7.60 (s, 1H); 7.77 (d, J = 8.7 Hz, 1H); 7.87 (s, 1H). MS (70 eV): 254 (55) [M$^{+\bullet}$]; 239 (100) [M$^{+\bullet}$ − Me]. **5a.** This ketone was prepared as a solid from 2,6-di-*tert*-butyl-4-methylnaphthalene according to the method used for synthesis of **3a**. It was used for the next step without further purification. ^{1}H NMR (CDCl$_3$): 1.38 (t, J = 7.5 Hz); 1.40 (s, 9H); 1.44 (s, 9H); 2.72 (s, 3H); 2.77 (s, 3H); 7.46 (d, J = 1.8 Hz, 1H); 7.89 (d, J = 1.5 Hz, 1H); 8.10 (d, J = 1.5 Hz, 1H); 8.35 (d, J = 1.5 Hz, 1H). **5b.** The diketone was prepared as described above for the desmethyl derivative, but THF was used (instead of Et$_2$O) for the condensation reaction. Yellow solid. Yield: 3.5 g (61%). ^{1}H NMR (CDCl$_3$): 1.39 (s,9H); 1.44 (d, J = 0.9 Hz, 9H); 2.77 (s, 3H); 6.09 (d, J = 4.5 Hz); 7.44 (s, 1H); 7.79 (s, 1H); 8.03 (s, 1H); 8.19 (s, 1H); 8.21 (d, J = 4.2 Hz, 1H). MS (70 eV): 324 (90) [M$^{+\bullet}$]; 309 (100) [M$^{+\bullet}$ - Me]; 281 (20); 267 (21); 239 (19); 165 (10); 57 (11). **5c.** Yellow solid. Yield: 3.1 g (96%). ^{1}H NMR (CDCl$_3$): 1.48 (s, 9H); 1.63 (s, 9H); 2.82 (s, 3H); 6.67 (d, J = 10.3 Hz, 1H); 7.53 (s, 1H); 8.31 (d, J = 2.1 Hz, 1H); 8.51 (d, J = 10.3 Hz, 1H); 8.81 (d, J = 2.1 Hz, 1H). **5-H:** NaBH$_4$ (1.0 g, 33 mmol) was added in small portions to the solution of **5c** (1.8 g, 5.9 mmol) and CeCl$_3$·7H$_2$O (2.24 g, 6 mmol) in 150 mL of MeOH at 0 °C. After the reaction mixture was stirred for 2 h at 0 °C, the solvent was evaporated and the residue was extracted with benzene (3 × 30 mL). Silica gel (15 g) was added to the combined extracts, and the solvent was evaporated. Column chromatography (50 g of silica gel) of the resulting solid material afforded three products. Evaporation of the first colorless fraction (hexane) and recrystallization of the residue from small amounts of hexane afforded colorless plates of phenalene (**5-H**). Yield: 0.5 g (29%), mixture of isomers. MS (70 eV): 291 (20) [M$^{+\bullet}$ − 1]; 290 (40) [M$^{+\bullet}$ − 2]; 276 (20) [M$^{+\bullet}$ − 1 − Me]; 235 (100). Next, the (deep blue) effluents gave 0.2 g (yield 6%) of coupling product **7** (X-ray structure shown in Figure 4). UV−vis (pentane, deep-blue solution): $\lambda_{max}(\epsilon)$ = 520 (15 000); 550 (53 000); 610 (110 000). UV−vis (KBr): $\lambda_{max}(\epsilon)$ = 550br, 600br. The third portion (benzene) afforded enone **5c** (43%). Radical **5$^\bullet$** was obtained as a colorless solution by the reduction of **5$^+$** B(C$_6$F$_5$)$_4^-$ with bis(pentamethylcyclopentadienyl)iron. ESR (10 mM in CH$_2$Cl$_2$): triplet of quintets, α = 1.7 G, α$_1$ = 1.9 G, α$_2$ = 6.0 G. Cation **5$^+$** B(C$_6$F$_5$)$_4^-$ was obtained as yellow crystals. Yield: 54%. ^{1}H NMR (CDCl$_3$): 1.58 (s, 9H); 1.85 (s, 9H); 3.29 (s, 3H); 8.19 (s, 1H); 8.19 (t, J = 7.8 Hz, 1H); 8.84 (d, J = 7.8 Hz, 1H); 8.98 (d, J = 2.0 Hz, 1H); 9.31 (d, J = 2.0 Hz, 1H); 9.70 (d, J = 7.8 Hz, 1H). **3-Ethyl-1,5-di-*tert*-butylphenalene (6-H)** was synthesized via the procedure described for the methyl derivative. Ethyl-di-*tert*-butylnaphthalene was prepared from 2,6-di-*tert*-butylnaphthalene (16 g, 67 mmol) by the same method as the methyl

derivative, but in this case diethyl sulfate was used to quench the Li-enolate. Yield: 12 g (57%) of white solid. ^{1}H NMR (CDCl$_3$): 1.38 (t, J = 7.5 Hz); 1.40 (s, 9H); 1.44 (s, 9H); 3.12 (q, J = 7.5 Hz, 2H); 7.37 (s, 1H); 7.53 (dd, J = 8.7, 2.1 Hz, 1H); 7.58 (s, 1H); 7.75 (d, J = 8.7 Hz, 1H); 7.92 (s, 1H). **6a.** ^{1}H NMR (CDCl$_3$): 1.38 (t, J = 7.5 Hz); 1.40 (s, 9H); 1.44 (s, 9H); 2.77 (s, 3H); 3.12 (q, J = 7.5 Hz, 2H); 7.45 (d, J = 1.8 Hz, 1H); 7.89 (d, J = 1.8 Hz, 1H); 7.89 (d, J = 1.5 Hz, 1H); 8.11 (d, J = 1.5 Hz, 1H); 8.36 (d, J = 1.5 Hz, 1H). MS (70 eV): 310 (35) [M$^{+\bullet}$]; 295 (100) [M$^{+\bullet}$ − Me]. **6b.** Yellow solid. ^{1}H NMR (CDCl$_3$): 1.38 (t, J = 7.5 Hz); 1.39 (s, 9H); 1.44 (d, J = 0.9 Hz, 9H); 3.12 (q, J = 7.5 Hz, 2H); 6.09 (d, J = 4.5 Hz, 1H); 7.46 (s, 1H); 7.78 (s, 1H); 8.10 (s, 1H); 8.20 (d+s, J = 4.5 Hz, 2H). **6c.** Yellow solid. ^{1}H NMR (CDCl$_3$): 1.43 (t, J = 7.5 Hz, 3H); 1.48 (s, 9H); 1.64 (s, 9H); 3.20 (q, J = 7.5 Hz, 2H); 6.66 (d, J = 10.0 Hz, 1H); 7.56 (s, 1H); 8.37 (d, J = 2.1 Hz, 1H); 8.52 (d, J = 10.0 Hz, 1H); 8.81 (d, J = 2.0 Hz, 1H). MS (70 eV): 320 (70) [M$^{+\bullet}$]; 305 (100) [M$^{+\bullet}$ − Me]. This material was used without further purification and **6-H** was obtained in low yield (12%), as colorless plates (hexane). MS (70 eV): 305 (25) [M$^{+\bullet}$ − 1]; 304 (40) [M$^{+\bullet}$-2]. Radical **6$^\bullet$** was obtained by oxidation of **6**-H (100 mg, 0.34 mmol) with chloranil (47 mg, 0.19 mmol). The ESR spectrum of **6$^\bullet$** showed a broadened quintet with parameters presented in Table 1. Cation **6$^+$** B(C$_6$F$_5$)$_4^-$. Yellow crystals. Yield: 45%. ^{1}H NMR (CDCl$_3$): 1.58 (s, 9H); 1.60 (t, J = 7.5 Hz, 3H); 1.86 (s, 9H); 3.60 (q, J = 7.5 Hz, 2H); 8.18 (t, J = 7.8 Hz, 1H); 8.22 (s, 1H); 8.84 (d, J = 7.8 Hz, 1H); 8.98 (d, J = 2.0 Hz, 1H); 9.32 (d, J = 2.1 Hz, 1H); 9.70 (d, J = 7.8 Hz, 1H).

ESR measurements were performed under an argon atmosphere from +20 to −90 °C in quartz ESR tubes equipped with Teflon valves. The intensity of the ESR signals (I_{EPR}) was determined by double integration of the averaged spectra after baseline correction. The fraction of monomer (α_M) in solution of **P$^\bullet$** was determined from the value of I_{EPR} that was normalized as described earlier (to account the temperature variation related to Curie law and instrumental factors).[10] The equilibrium constant was calculated as: $K_D = (1 - \alpha_M)/2c_o\alpha_M^2$, where c_o is the overall concentration of **P$^\bullet$** added to the solution; and the thermodynamic parameters for dimerization were calculated by the least-squares procedure from the dependence of ln(K_D) with $1/T$.

Electronic spectroscopy was carried out on a Dewar equipped with quartz windows. The cell was equipped with a Teflon valve fitted with Viton O-rings as described earlier.[10]

X-ray Crystallography. The diffraction data were collected with the aid of a diffractometer equipped with a CCD detector using MoK_α radiation (λ = 0.71073 Å), either at −150 or at −100 °C. In all cases, semiempirical absorption correction was applied. The structures were solved by direct methods and refined by full matrix least-squares procedure (see Table S1 (Supporting Information) for crystallographic data). [The X-ray structure details of various compounds have been deposited with the Cambridge Crystallographic Data Centre, U.K., and can be obtained, on request, from the CCDC.]

Supporting Information Available: Crystallographic parameters and the details of the structure refinements, X-ray structures of phenalene precursor **3-H** and cationic salt $3^+B(C_6F_5)_4^-$, temperature dependence of ESR spectrum intensity for radical **1$^\bullet$**, NIR absorption band of cation-radical dimer $3_2^{\bullet+}$, X-ray structure of cationic salt $4^+B(C_6F_5)_4^-$, and ESR spectrum of **4$^\bullet$**. This material is available free of charge via the Internet at http://pubs.acs.org.

JO051612A